state below T_N (as might be inferred from the neutron data[5]). The far-infrared data, which suffer less from instrumental limits on the resolution, indicate, however, a rather dramatic increase in linewidth which dominates the results of the theory and produces the opposite effect—a line broadening at the Néel point. Although the basic idea proposed by Mills and Ushioda may be correct, in its present form it does not appear to properly describe the experimental results.

[31]P. L. Richards, J. Opt. Soc. Am. 54, 1474 (1964).

[32]R. M. MacFarlane and S. Ushioda, Solid State Commun. 8, 1081 (1970); R. M. MacFarlane, Phys. Rev. Letters 25, 1454 (1970).

[33]S. P. S. Porto, P. A. Fleury, and T. C. Damen, Phys. Rev. 154, 522 (1967).

[34]H. M. Gladney, Phys. Rev. 146, 253 (1966).

[35]P. S. Narayanan, Proc. Indian Acad. Sci. 32A, 279 (1950).

[36]J. M. Ziman, *Electrons and Phonons* (Oxford U. P., London, 1960), p. 16f.

[37]G. Parisot, S. J. Allen, Jr., R. E. Dietz, H. J. Guggenheim, R. Moyal, P. Moch, and C. Dugautier, J. Appl. Phys. 41, 890 (1970).

[38]L. F. Johnson, R. E. Dietz, and H. J. Guggenheim, Appl. Phys. Letters 5, 21 (1964).

[39]H. M. Gladney, Phys. Rev. 143, 198 (1966).

[40]This is true for magnetic fields in either the x or y direction. It must be noted that the two sites in CoF_2 differ by a rotation of 90°. Consequently, when a field is applied in the x direction, the magnetization on the site in question is proportional to g_x^2 but the magnetization on the opposite side will be proportional to g_y^2.

[41]We have tacitly assumed that the spin-phonon coupling in Co^{2+}, MgF_2 does not significantly perturb the 157-cm^{-1} splitting. Since the energy separation of this state and the E_g phonon is five times larger in MgF_2 than in CoF_2, we expect that it may perturb the excited doublet of Co^{2+} in MgF_2 by no more than ~ 3 cm^{-1} ($\sim 2\%$). We choose to ignore such a correction.

[42]E. Belorizky, S. C. Ng, and T. G. Phillips, Phys. Rev. 181, 467 (1969).

PHYSICAL REVIEW B VOLUME 4, NUMBER 3 1 AUGUST 1971

Magnetic Excitations in Antiferromagnetic CoF_2. II. Uniform Magnetic Excitations near $T = 0$ °K

S. J. Allen, Jr. and H. J. Guggenheim
Bell Telephone Laboratories, Murray Hill, New Jersey 07974

(Received 11 January 1971)

Far-infrared absorption experiments on CoF_2 at 4.2 °K are extended to include all the uniform magnetic excitations below 300 cm^{-1}. The linear and nonlinear Zeeman effect, obtained with externally applied magnetic fields parallel and perpendicular to the spin direction, are also observed. A model of the uniform magnetic excitations derived from an effective $S = \frac{3}{2}$, Co^{2+} manifold is constructed by including a large orthorhombic anisotropy field, determined from Co^{2+} in MgF_2, a simple isotropic bilinear exchange, and the independently determined spin-phonon coupling to the E_g optical phonon. The model gives a satisfactory account of the energies, linear and nonlinear Zeeman effect, as well as the absorption intensities.

I. INTRODUCTION

In the preceding paper the coupling between the Co^{2+} effective $S = \frac{3}{2}$ spin and the E_g optical phonon was discussed at length—the object being to extract from the temperature dependence of transferred magnetic-dipole intensity some microscopic parameters describing the spin-lattice interaction. In the present discussion, we focus our attention on the spin system and attempt to derive a quantitative description of the uniform, $k = 0$, magnetic excitations at $T = 0$ °K that evolve from the effective $S = \frac{3}{2}$ manifold. Experimentally we have extended the far-infrared absorption experiments of Barker and Ditzenberger[1] as well as Richards[2] to include all the uniform magnetic excitations of the system at 4.2 °K below 300 cm^{-1}. The Zeeman effect both parallel and perpendicular to the spin axis is obtained. The work confirms the $k = 0$ excitation energies obtained by neutron diffraction[3] and agrees with recent Raman scattering experiments by MacFarlane.[4]

The spectrum of excitations that evolve from the Co^{2+} ion when it is found in a concentrated salt such as CoF_2 may be viewed from two points of view. In the first case one may consider all but the lowest excitation to be excitons, perturbed to a greater or lesser extent by the Co^{2+}-Co^{2+} interactions, while the lowest excitation is a spin wave. It is distinguished from the excitons only by the fact that in the absence of Co^{2+}-Co^{2+} interactions the spin waves have zero excitation energy while the excitons retain a finite energy. With reference to Fig. 1, for instance, the 12 levels derived from the $^4\Gamma_4$ in the ordered state will contribute eleven single-particle-like excitations to the collective

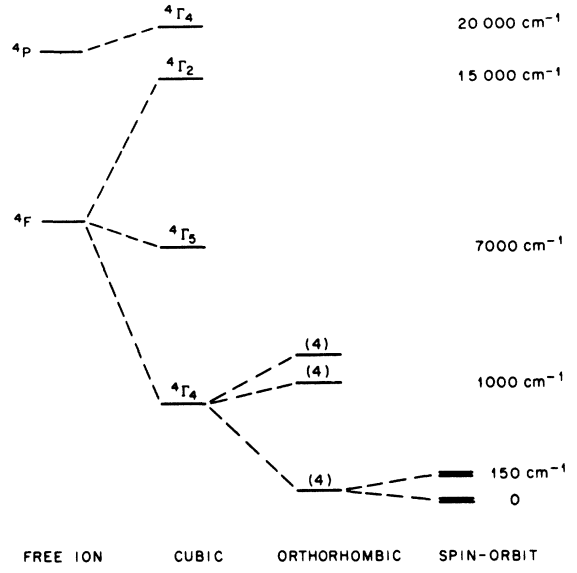

FIG. 1. Crystal-field splitting of the d^7 manifold by the orthorhombic crystal field (Ref. 10).

spectrum in the condensed salt but only the lowest excitation derived from ground-state Kramers doublet will go to zero energy as we turn off the Co-Co interaction. This is, of course, a legitimate point of view provided that the interactions between the spin-wave branch and the excitons at ~150 cm^{-1} are properly included.

The second point of view makes the following distinction between the excitons. We treat the excitons that derive from the levels near 150 cm^{-1} as different from those excitations near ~1000 cm^{-1}. Although the distinction may seem somewhat arbitrary, it is useful for the following reasons. The exchange interactions appreciably mix the lowest Kramers doublet with the first excited doublet but clearly are ineffective in mixing with the levels at 1000 cm^{-1}. Consequently, treating all the excitons on an equal footing makes the problem unnecessarily burdensome. Further, if we should consider the limiting case where the orthorhombic crystal field is large enough to completely quench the orbital motion, the excited states at 1000 cm^{-1} move to arbitrarily high energies whereas the lowest four levels coalesce into a simple spin-$\frac{3}{2}$ quartet. Hence, physically, we may think of the lowest four states as being $S=\frac{3}{2}$ spin states with appreciable ($\lambda^2/E^2 \sim 0.1$) but not overwhelming admixture of orbital motion that lifts the degeneracy by ~150 cm^{-1}. This point of view further suggests the following interesting conceptual problem. How do we describe the spin excitations in ordered systems as we gradually increase the local anisotropy field from the usual limit where anisotropy field/exchange field $\ll 1$ to the case where they are comparable and finally to the limit anisotropy/exchange >1, the case in CoF_2? Silberglitt and Torrance[5] have recently noted that a new type of two-magnon bound state may appear in ferromagnets with $S \geq 1$ as the anisotropy field is increased with respect to the exchange field. The excitations that evolve from transitions to the doublet at 150 cm^{-1} are in fact examples of such a single-ion two-magnon bound state in the limit where the anisotropy energy ~3 × (exchange energy). However, the discussion can proceed in a relatively straightforward manner, since they appear to always lie outside the continuum of two-magnon excitations derived exclusively from the lowest Kramers doublet. We take the point of view then that we are dealing with an effective $S=\frac{3}{2}$ antiferromagnet in the presence of an anisotropy field large compared with the exchange. The excited states near 1000 cm^{-1} are not explicitly considered in the treatment that follows.

There have been a number of earlier discussions of the magnetic excitations of CoF_2. Kamimura[6] first calculated the spin-wave branch by treating only the lowest Kramers doublet but included an anisotropic exchange between effective $S=\frac{1}{2}$ spins. Lines[7] made considerable improvement by including the exchange mixing of the two lowest doublets by the molecular field and obtained a good fit to the lowest branch. With the exception of Ishikawa and Moriya,[8] attempts to straightforwardly extend Lines's approach to the excitations derived from first excited doublet have been successful only from a qualitative point of view.[3] Ishikawa and Moriya have recently calculated the excitation spectra for CoF_2 and have obtained reasonably good agreement with the energies of the uniform excitations, but have neglected the strong interaction of the transverse modes with the E_g phonon.[9] In the present paper we have calculated the uniform magnetic excitations at $T=0$ °K including the spin-phonon coupling and have also obtained the linear and nonlinear Zeeman effects for applied fields parallel and perpendicular to the spin axis. The results obtained with this model agree reasonably well with the experimental results.

In Sec. II the model for the low-lying excitations is developed, the resulting Hamiltonian put forward and diagonalized with suitable approximations at $T=0$ °K. Section III summarizes the experimental results while Sec. IV attempts to reconcile the model predictions and experimental results. Section V is reserved for final discussion.

II. THEORY

A model for the magnetic excitations in CoF_2 is constructed from the following simple minded point of view. We first assume that all the single-ion properties can be taken from Co^{2+} in some suitable diamagnetic isomorph and described by an effective

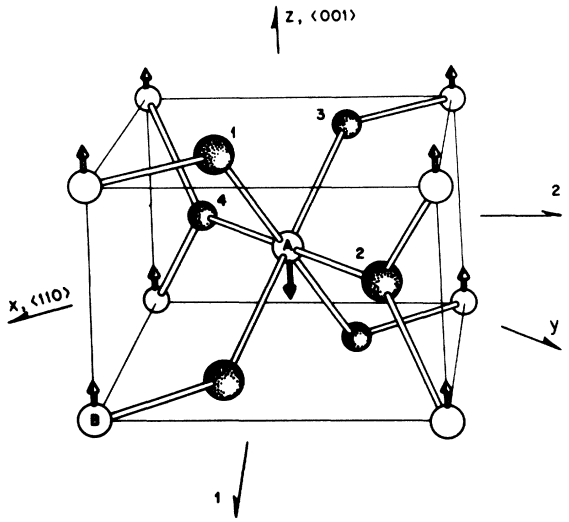

FIG. 2. CoF_2 crystal structure showing magnetic ordering below 37.7 °K (Ref. 10).

$S=\frac{3}{2}$ spin Hamiltonian including terms no higher than second order in the spin. Second, we assume a simple isotropic bilinear exchange between the $S=\frac{3}{2}$ spins. This requires some justification. The only complication that is introduced is the spin-phonon coupling to E_g optical phonon. With these ingredients we first put forward the spin Hamiltonian and indicate how it is diagonalized for an arbitrarily directed magnetic field. We pay special attention to the longitudinal excitations which experience a Davydov splitting. These modes are not coupled to the E_g phonon and can be used to extract an exchange parameter.

The magnetic crystal structure of CoF_2 is shown in Fig. 2.[10] It consists of two magnetic sublattices with magnetic moments parallel and antiparallel to the c axis. The Co^{2+} ion is surrounded by an orthorhombically distorted octahedron of F^- ions.[11] The local symmetry at the two possible sites is identical if one rotates the octahedron by 90° about the c axis as one passes from the body center to the corner of the unit cell.

A. Truncated Spin and Lattice Hamiltonian

The collective magnetic excitations below 300 cm^{-1} in CoF_2 are assumed to evolve entirely from lowest four levels of the Co^{2+} ion found in a suitable diamagnetic isomorph. This appears to be a reasonable assumption for the next levels are approximately[11,12] 1000 cm^{-1} above the ground state and the ion pair interactions which distinguish the concentrated salt from the isolated Co^{2+} ion are only of the order of 50 cm^{-1}.[7] This is not to say, of course, that there is no appreciable mixing of the lowest four levels with the higher eight levels by the spin-orbit interactions and the orthorhombic crystal field. These are, indeed, quite large. But they are purely single-ion effects and may be included in a suitable single-ion spin Hamiltonian. For the body-centered site shown in Fig. 2, we write for the single ion an effective $S=\frac{3}{2}$ Hamiltonian:

$$-\delta S_z^2+\gamma(S_x^2-S_y^2)+g_x S_x H_x+g_y S_y H_y+g_z S_z H_z\ . \qquad (1)$$

The corner sites are obtained by rotating about the z axis by 90°. All the interactions with the external magnetic field are assumed to be described in (1). It should also be noted, that in transplanting the single-ion parameters determined from Co^{2+} in MgF_2, we tacitly assume that there is no dynamic spin-optic phonon coupling of consequence in the diamagnetic isomorph. Although the matrix element connecting the exciton and phonon state must be nearly the same in Co^{2+}:MgF_2 as it is in CoF_2, in retrospect, we note that the energy separation between exciton and phonon is five times greater in Co^{2+} MgF_2 than in CoF_2. This leads one to estimate that the single-ion crystal-field splitting of Co^{2+} in MgF_2 is perturbed by only 3 cm^{-1} by the dynamic spin-lattice interaction with the E_g phonon. We do not include these corrections here. The assumption then is that exchange effects *alone* do not appreciably mix the ground $S=\frac{3}{2}$ manifold with the higher states and that the single-ion Hamiltonian is given by (1).

The exchange interaction need not act alone, however, between the ground-state manifold and the other states. The spin-orbit interaction taken with the exchange interaction can alter the nature of the exchange interactions in the ground state.[13] These appear as multipole-multipole spin interactions, the largest of which is the Moriya-Dzialoshinski[14] antisymmetric exchange and is of the order of $(\lambda/E)J\vec{i}_d\cdot\vec{S}_A\times\vec{S}_B$ where λ/E is the ratio of spin-orbit energy to the energy of the excited orbital states and is approximately 0.3. Fortunately the antisymmetric terms are of no consequence as long as we restrict our attention to the uniform excitations of the system. The next important multipole-multipole interactions which do influence the uniform response of the system are dipole-octupole, quadrupole-quadrupole, and anisotropic, symmetric, bilinear exchange which all appear in third order. They are of the order $(\lambda^2/E^2)J\sim 0.09J$. However, restricting our discussion again to the uniform response of the system further reduces the estimate. It is shown in Appendix A that at $k=0$ the coefficients of these third-order terms (second order in λ and first order in J) actually appear as differences between the various off-diagonal exchange parameters. Following Ishikawa and Moriya's[8] suggestion that these ex-

change parameters should differ from one another by no more than 30% reduces the magnitude of these terms to $0.3\lambda^2/E^2J \sim 0.03J$ and hence they are relatively unimportant. In the discussion that follows then, we assume that only an isotropic exchange interaction, between effective $S=\frac{3}{2}$ spins on the body-center and corner sites, is required. The exchange interaction between the spins on the same sublattice along the c axis is also ignored. We take as our final justification for these simplifying approximations the relatively good quantitative agreement obtained with experiment, while recognizing that the remaining discrepancies may in part be due to these assumptions.

The third interaction that we consider in constructing the Hamiltonian for the system is the spin-lattice interaction. This may be separated into two parts—exchange striction and magnetostriction. Exchange striction is ignored throughout. It should be no larger in CoF_2 than in the other transition-metal fluorides and does not significantly alter the spectrum of spin excitations. Magnetostrictive effects are produced by modulation of crystal field by the lattice distortion and do play an important role in the magnetic excitations. As discussed in the preceding paper, we consider only distortions which transform locally about the Co^{2+} like the zx and zy shears. We must further distinguish, however, two types of distortion, the internal and external or macroscopic distortion.[15] The internal distortion only moves the atoms within the unit cell—it does not distort the bravais lattice. The macroscopic or external distortion distorts the entire lattice uniformly. It is in fact the strain produced by an applied laboratory stress. Clearly a static uniform external strain produces a static internal distortion; however, a high-frequency phonon at $k=0$ which is a pure internal distortion does not produce a corresponding macroscopic external strain of the same symmetry. As a result, it is important to point out that the experiment described in the preceding paper determines the coupling to the internal distortions alone and does not tell us what the *static* magnetoelastic coupling constants are.[16] Consequently although we may use the spin-lattice coupling parameters determined in the preceding paper to calculate the excitation spectra, they do not help us determine the magnetoelastic ground state when we produce a static distortion by applying a magnetic field perpendicular to the c axis. However, it is shown in Appendix B that the nonlinear Zeeman effect produced by applying the magnetic field perpendicular to the spin direction is not significantly affected by the magnetoelastic coupling—the errors introduced being less than the errors in the perpendicular g factors used in the calculations— and as a result the magnetoelastic effects on the perpendicular Zeeman effect are ignored. The *dynamic* spin-lattice coupling to the internal distortions is included for it appreciably alters the spectrum of spin excitations.

The above approximations and assumptions are gathered in the following Hamiltonian describing the low-lying magnetic excitations:

$$\sum_i \{-\delta S_z^A(i)^2+\gamma[S_x^A(i)^2-S_y^A(i)^2]-\delta S_z^B(i)^2-\gamma[S_x^B(i)^2-S_y^B(i)^2]+g_z[S_z^A(i)+S_z^B(i)]H_z$$

$$+[g_x S_x^A(i)+g_y S_x^B(i)]H_x+[g_y S_y^A(i)+g_x S_y^B(i)]H_y\}\sum_i\sum_{\vec{\Delta}} J\vec{S}^A(i)\cdot\vec{S}^B(i,\vec{\Delta})+\frac{1}{N^{1/2}}\sum_i\sum_{\vec{k}}\sum_p j(\alpha_{\vec{k},p}-\alpha^\dagger_{-\vec{k},p})\left(\frac{\hbar}{2m\omega_{\vec{k},p}}\right)^{1/2}$$

$$\times\{[\eta Q_{zx}^A(i)f_{\vec{k},p}^{1,3}+\xi Q_{zx}^B(i)g_{\vec{k},p}^{1,3}]+[\eta Q_{zy}^B(i)f_{\vec{k},p}^{2,4}+\xi Q_{zy}^A(i)g_{\vec{k},p}^{2,4}]\}+\sum_{\vec{k}}\sum_p \hbar\omega_{\vec{k},p}\alpha^\dagger_{\vec{k},p}\alpha_{\vec{k},p}\,. \qquad (2)$$

In the above the first terms represent the single-ion effects produced by the crystal field and the external magnetic field. The second is the simplest form of exchange that could be introduced between the next-nearest-neighbor spins—an isotropic Heisenberg exchange. $\vec{\Delta}$ runs over the body corner sites. The third term is the spin-phonon coupling used in the preceding paper, where we have replaced the phonon displacement operator $X_{\vec{k},p}$ with the combination of phonon operators $j(\alpha_{\vec{k},p}-\alpha^\dagger_{-\vec{k},p})\times(\hbar/2m\omega_{\vec{k},p})^{1/2}$. The last term is the energy of the $\vec{k},p$ phonon.

B. Diagonalizing the Hamiltonian

Diagonalization of the Hamiltonian proceeds in a manner similar to that described by Grover,[17] and subsequently used by Cowley *et al.*[3] It is a logical extension of Lines's[7] approach to CoF_2.

We diagonalize the Hamiltonian (2) by first finding a self-consistent molecular field ground state at $T=0\,^\circ K$ for an arbitrarily directed external magnetic field. This is done by an iterative procedure which first finds the ground state on the A sites produced by the following Hamiltonian:

$$H=-\delta(S_z^A)^2+\gamma[(S_x^A)^2-(S_y^A)^2]+zJ\langle\vec{S}^B\rangle\vec{S}^A+g_z H_z S_z^A+g_x H_x S_x^A+g_y H_y S_y^A\,. \qquad (3)$$

The initial value chosen for $\langle\vec{S}^B\rangle$ may be taken as $-\frac{3}{2}\vec{i}_z$. The value for $\langle\vec{S}^A\rangle$ found for the ground state

of the above Hamiltonian is then simply used in a similar Hamiltonian for $\vec{S}^B$:

$$H = -\delta(S_z^B)^2 - \gamma[(S_x^B)^2 - (S_y^B)^2] + zJ\langle\vec{S}^A\rangle\vec{S}^B + g_z H_z S_z^B + g_x H_y S_y^B + g_y H_x S_x^B \ . \quad (4)$$

The procedure is repeated by using the $\langle\vec{S}^B\rangle$ found from the ground state of (4), and substituting into (3), generating a new $\langle\vec{S}^A\rangle$. The iteration converges for the parameters used, to the known spin structure for $\vec{H}=0$. In the actual calculations, which were done on a computer, self-consistency was considered achieved if the calculated spin values differed by no more than 10^{-3} from the input values.

As previously mentioned, for applied magnetic fields perpendicular to the spin direction, static quadrupole moments Q_{zx} and Q_{xy} will be generated which will produce at least local distortions of the lattice. These static distortions of the lattice will lower the electronic free energy and rigorously should be included in the calculation of the ground state. It is shown, however, in Appendix B that this produces only 5% effects on the g factors for magnetic fields perpendicualr to the spin axis, hence these magnetoelastic effects are not included in the ground-state calculation.

The ground-state calculation simultaneously generates three excited-state energy levels and wave functions of each Co^{2+} site which can then be used as a basis for calculating the collective excitations at $T=0\,^\circ$K. The four levels on the A site in the ith unit cell may be labeled $|i,A,n\rangle$ where n goes from 0 to 3. $|i,A,0\rangle$ is taken as the ground state. A set of local creation and destruction operators is denoted by $\{a_{i,n}^\dagger,\ a_{i,n},\ b_{i,n}^\dagger,\ b_{i,n}\}$. In the local representation which diagonalizes (3), $a_{i,n}^\dagger$ would take the following form for $n=2$:

$$a_{i,2}^\dagger = \begin{pmatrix} 0&0&0&0\\ 0&0&0&0\\ 1&0&0&0\\ 0&0&0&0 \end{pmatrix} \ . \quad (5)$$

These operators satisfy the following commutation rules:

$$[a_{i,n}, b_{j,m}] = 0, \quad [a_{i,n}^\dagger, b_{j,m}] = 0, \quad (6)$$

and

$$[a_{i,n}, a_{j,m}^\dagger] = \delta_{i,j}\left[-a_{j,m}^\dagger a_{i,n} + \delta_{m,n}\left(1 - \sum_{p\neq n} a_{j,p}^\dagger a_{j,p}\right)\right] \ . \quad (7)$$

If the molecular field ground state is a good approximation to the final ground state then

$$\langle|\,[a_{i,n}, a_{j,m}^\dagger]\,|\rangle = \delta_{i,j}\left[-\langle|\,a_{j,m}^\dagger a_{j,n}\,|\rangle + \delta_{m,n}\left(1 - \sum_{p\neq n}\langle|\,a_{j,p}^\dagger a_{j,p}\,|\rangle\right)\right] \approx \delta_{i,j}\delta_{m,n} \quad (8)$$

and we may approximate the operators so defined by bosons.

The local spin operators may be expressed as a quadratic function of these operators as follows:

$$\vec{S}^A(i) = \langle 0|\vec{S}^A|0\rangle + \sum_{n=1}^{3}[\langle n|\vec{S}^A|n\rangle - \langle 0|\vec{S}^A|0\rangle]a_{i,n}^\dagger a_{i,n} + \sum_{n=1}^{3}\langle n|\vec{S}^A|0\rangle a_{i,n}^\dagger + \langle 0|\vec{S}^A|n\rangle a_{i,n} + \sum_{n=1}^{3}\sum_{m>n}^{3}\langle m|\vec{S}^A|n\rangle a_{i,m}^\dagger a_{i,n} + \langle n|\vec{S}^A|m\rangle a_{i,n}^\dagger a_{i,m} \ , \quad (9)$$

where the matrix-element coefficients are determined in the representation diagonalizing the self-consistent molecular field Hamiltonians (3) and (4). Similarly we may write the quadrupole operators Q_{zx} and Q_{xy} as a suitable combination of these local quasiboson operators.

The interactions between the Co^{2+} sites and its neighboring sites as well as the E_g phonons, that were not included in the molecular field treatment, are now added to the Hamiltonians (3) and (4) to reproduce the original Hamiltonian (2):

$$H = \sum_i \{-\delta S_z^A(i)^2 + \delta[S_x^A(i)^2 - S_y^A(i)^2] + zJ\langle\vec{S}^B\rangle\cdot\vec{S}^A(i) - \delta S_z^B(i)^2 - \gamma[S_x^B(i)^2 - S_y^B(i)^2] + zJ\langle\vec{S}^A\rangle\cdot\vec{S}^B(i) + g_z[S_z^A(i) + S_z^B(i)]H_z + [g_x S_x^A(i) + g_y S_x^B(i)]H_x + [g_y S_y^A(i) + g_x S_y^B(i)]H_y\} + \sum_i\sum_{\vec{\Delta}} J[\vec{S}^A(i) - \langle\vec{S}^A\rangle]\cdot[\vec{S}^B(i,\vec{\Delta}) - \langle\vec{S}^B\rangle] - \sum_i zJ\langle\vec{S}^A\rangle\cdot\langle\vec{S}^B\rangle + \frac{1}{N^{1/2}}\sum_i\sum_{\vec{k}}\sum_p j(\alpha_{\vec{k},p} - \alpha_{-\vec{k},p}^\dagger)\left(\frac{\hbar}{2m\omega_{\vec{k},p}}\right)^{1/2} \times\{[\eta Q_{zx}^A(i) f_{\vec{k},p}^{1,3} + \xi Q_{zx}^B(i) g_{\vec{k},p}^{1,3}] + [\eta Q_{xy}^B(i) f_{\vec{k},p}^{2,4} + \xi Q_{xy}^A(i) g_{\vec{k},p}^{2,4}]\} + \sum_{\vec{k}}\sum_p \hbar\omega_{\vec{k},p}\alpha_{\vec{k},p}^\dagger\alpha_{\vec{k},p} \ . \quad (10)$$

The first summation in the above is recognized as the molecular field Hamiltonians (3) and (4) and is immediately replaced by

$$\sum_i\sum_{n=1}\epsilon_n^A a_{i,n}^\dagger a_{i,n} + \epsilon_n^B b_{i,n}^\dagger b_{i,n} \ , \quad (11)$$

where the ϵ_n^A and ϵ_n^B are the energies obtained from

the molecular field. The second sum, representing the off-diagonal interactions or transfer of excitation from one site to the next, contains terms through fourth order in the creation and destruction operators. We keep, however, only the bilinear terms in the present calculation. In general, for arbitrarily oriented external magnetic fields, we have

$$J\sum_{i}\sum_{\vec{\Delta}}\left(\sum_{n=1}^{3}\langle n|\vec{S}^{A}|0\rangle a_{i,n}^{\dagger}+\langle 0|\vec{S}^{A}|n\rangle a_{i,n}\right)\times\left(\sum_{n=1}^{3}\langle n|\vec{S}^{B}|0\rangle b_{i,\vec{\Delta},n}^{\dagger}+\langle 0|\vec{S}^{B}|n\rangle b_{i,\vec{\Delta},n}\right). \quad (12)$$

Similarly in the spin-phonon interaction term, we replace the quadrupole operators with expressions like

$$Q_{zx}^{A}(i)=\sum_{n=1}^{3}\langle n|Q_{zx}^{A}|0\rangle a_{i,n}^{\dagger}+\langle 0|Q_{zx}^{A}|n\rangle a_{i,n}. \quad (13)$$

We may now Fourier transform the boson operators $a_{i,n}$ and $b_{i,n}$ to obtain plane-wave excitations of the system $a_{\vec{k},n}$ and $b_{\vec{k},n}$:

$$a_{i,n}=\frac{1}{N^{1/2}}\sum_{\vec{k}}e^{i\vec{k}\cdot\vec{r}_i}a_{\vec{k},n}. \quad (14)$$

Upon substitution of the above transformation as well as the expressions (11)–(13) into (10) and restricting our attention to $\vec{k}=0$, we obtain for the Hamiltonian

$$\begin{aligned}H=&\sum_{n=1}^{3}\epsilon_n^{A}a_{0,n}^{\dagger}a_{0,n}+\epsilon_n^{B}b_{0,n}^{\dagger}b_{0,n}+zJ\left(\sum_{n=1}^{3}\langle n|\vec{S}^{A}|0\rangle a_{0,n}^{\dagger}+\langle 0|\vec{S}^{A}|n\rangle a_{0,n}\right)\left(\sum_{m=1}^{3}\langle m|\vec{S}^{B}|0\rangle b_{0,n}^{\dagger}+\langle 0|\vec{S}^{B}|m\rangle b_{0,n}\right)\\&+j(\alpha_{0,E_g,zx}-\alpha_{0,E_g,zx}^{\dagger})\left(\frac{\hbar}{2m\omega_{0,E_g}}\right)^{1/2}\eta\sum_{n=1}^{3}(\langle n|Q_{zx}^{A}|0\rangle a_{0,n}^{\dagger}+\langle 0|Q_{zx}^{A}|n\rangle a_{0,n})\\&+\xi\sum_{m=1}^{3}(\langle m|Q_{zx}^{B}|0\rangle b_{0,m}^{\dagger}+\langle 0|Q_{zx}^{B}|m\rangle b_{0,m})+j(\alpha_{0,E_g,zy}-\alpha_{0,E_g,zy})\left(\frac{\hbar}{2m\omega_{0,E_g}}\right)^{1/2}\\&\times\left[\sum_{n=1}^{3}(\langle n|Q_{zy}^{A}|0\rangle a_{0,n}^{\dagger}+\langle 0|Q_{zy}^{A}|n\rangle a_{0,n})+\eta\sum_{m=1}^{3}(\langle m|Q_{zy}^{B}|0\rangle b_{0,m}^{\dagger}+\langle 0|Q_{zy}^{B}|m\rangle b_{0,m})\right]\\&+\hbar\omega_{0,E_g}(\alpha_{0,E_g,ax}^{\dagger}\alpha_{0,E_g,zx}+\alpha_{0,E_g,zy}^{\dagger}\alpha_{0,E_g,zy}). \quad (15)\end{aligned}$$

This Hamiltonian can be straightforwardly diagonalized by making a transformation[18] of the following form:

$$\begin{aligned}x_l=&\sum_{n=1}^{3}(u_{n,l}^{*}a_{0,n}-v_{n,l}^{*}a_{0,n}^{\dagger})+\sum_{m=1}^{3}(u_{m,l}^{*}b_{0,m}-v_{m,l}^{*}b_{0,m}^{\dagger})\\&+(u_{zx,l}^{*}\alpha_{0,E_g,zx}-v_{zx,l}^{*}\alpha_{0,E_g,zx}^{\dagger})\\&+(u_{zy,l}^{*}\alpha_{0,E_g,zy}-v_{zy,l}^{*}\alpha_{0,E_g,zy}^{\dagger}), \quad (16)\end{aligned}$$

where x_l satisfies the equation

$$[H,x_l]=-E_l x_l. \quad (17)$$

The eigenvalue problem produced by magnetic fields in the $\langle 100\rangle$ direction requires finding the eigenvectors and eigenvalues of a complex *non*-Hermitian 16×16 matrix. This is done most conveniently by computer using a nonsymmetric matrix package which was kindly provided by Businger.[19]

In summary then the program is as follows. A self-consistent molecular field ground state ignoring static magnetoelastic effects is found for an arbitrarily oriented magnetic field. The resulting energies and wave functions are used to construct a set of local quasiboson operators which are introduced to describe the off-diagonal interactions between Co^{2+} ions and between the Co^{2+} ion and the E_g phonon. The Hamiltonian is bilinearized and the eigenvalues and eigenvectors found from the equations of motion on the computer. The results for zero applied magnetic field are shown schematically in Fig. 3. At high temperatures (no molecular field), each site contains two Kramers doublets separated by ~ 157 cm^{-1}. We first apply a molecular field lifting the degeneracy and producing four levels on each site. At $T=0$ °K there are three distinct excitations from the ground state which form the basis for describing the collective excitation. The six excitations per unit cell then give six uniform, $k=0$, "single-particle" excitations at $T=0$ °K. These are also shown schematically in Fig. 3. There are two pairs of transverse excitations transforming like $\Gamma_3^{+}+\Gamma_4^{+}$. (That is, they are polarized like S_x and S_y.) In addition, we show the E_g phonon which transforms like $\Gamma_3^{+}+\Gamma_4^{+}$. There are two longitudinal magnetic excitations, Γ_1^{+} and Γ_2^{+} (S_z polarization), that experience a magnetic Davydov splitting.[20]

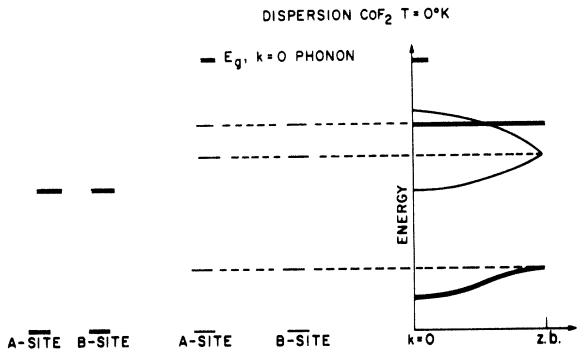

FIG. 3. Schematic of the evolution of the CoF_2 magnetic excitations from the two Kramers doublets in the paramagnetic state to the collective behavior in the ordered state at $T = 0$ °K.

C. Longitudinal Spin-Excitations-Davydov Splitting

We now consider explicitly the longitudinal excitations of the system that suffer a Davydov splitting. In the absence of an applied field, these modes do not interact with the E_g phonons and therefore can be used to extract the exchange parameter zJ unambiguously from the experiments. In zero applied field the molecular field Hamiltonian that we solve has the following form for the A sites:

$$-\delta(S_z^A)^2+\gamma[(S_x^A)^2-(S_y^A)^2]-\alpha S_z^A\ , \tag{18}$$

where $\alpha=-zJ\langle S_z^B\rangle$ and we note that in this case $|\langle S_z^B\rangle| = |\langle S_z^A\rangle|$. The resulting eigenvalues and eigenvectors[7] are

$$\begin{aligned}
E_3&=-\tfrac{5}{4}\delta+\tfrac{1}{2}\alpha+[(\alpha-\delta)^2+3\gamma^2]^{1/2}\ ,\\
E_2&=-\tfrac{5}{4}\delta-\tfrac{1}{2}\alpha+[(\alpha+\delta)^2+3\gamma^2]^{1/2}\ ,\\
E_1&=-\tfrac{5}{4}\delta+\tfrac{1}{2}\alpha-[(\alpha-\delta)^2+3\gamma^2]^{1/2}\ ,\\
E_0&=-\tfrac{5}{4}\delta-\tfrac{1}{2}\alpha-[(\alpha+\delta)^2+3\gamma^2]^{1/2}
\end{aligned} \tag{19}$$

and

$$|3\rangle=d|-\tfrac{3}{2}\rangle-c|\tfrac{1}{2}\rangle\ ,\quad |2\rangle=b|\tfrac{3}{2}\rangle-a|-\tfrac{1}{2}\rangle\ , \tag{20}$$

$$|1\rangle=c|-\tfrac{3}{2}\rangle+d|\tfrac{1}{2}\rangle\ ,\quad |0\rangle=a|\tfrac{3}{2}\rangle+b|-\tfrac{1}{2}\rangle\ ,$$

where

$$\frac{a}{b}=-\frac{[(\alpha+\delta)^2+3\gamma^2]^{1/2}+\alpha+\delta}{\sqrt{3}\,\gamma}\ ,$$

$$\frac{c}{d}=-\frac{[(\alpha-\delta)^2+3\gamma^2]^{1/2}-\alpha+\delta}{\sqrt{3}\,\gamma}\ . \tag{21}$$

For the longitudinal modes we need only consider the ground state $|0\rangle$ and the excited state $|2\rangle$. The energy separation we denote by

$$\epsilon_2=E_2-E_0=2[(\alpha+\delta)^2+3\gamma^2]^{1/2}\ . \tag{22}$$

The coupling between sites is provided by the S_z matrix element which in second-quantized form becomes

$$S_z^A=\langle 2|S_z|0\rangle(a_2+a_2^\dagger)\ , \tag{23}$$

where

$$\langle 2|S_z|0\rangle=2ab\ . \tag{24}$$

For S_z^B we have simply

$$\langle 2|S_z^B|0\rangle=-\langle 2|S_z^A|0\rangle\ . \tag{25}$$

Then we have

$$\begin{aligned}
S_z^A&=2ab(a_2+a_2^\dagger)\ ,\\
S_z^B&=-2ab(b_2+b_2^\dagger)
\end{aligned} \tag{26}$$

and for the Hamiltonian

$$H=\epsilon_2 a_2^\dagger a_2+\epsilon_2 b_2^\dagger b_2 - zJ(2ab)^2(a_2+a_2^\dagger)(b_2+b_2^\dagger)\ .$$

The Hamiltonian is diagonalized by the following transformations:

$$\begin{aligned}
X_1&=C_1^1(a_2+b_2)+C_2^1(a_2^\dagger+b_2^\dagger)\ ,\\
X_2&=C_1^2(a_2-b_2)+C_2^2(a_2^\dagger-b_2^\dagger)\ ,
\end{aligned} \tag{27}$$

where

$$\frac{C_1^1}{C_2^1}=\frac{zJ(2ab)^2}{[\epsilon_2{}^2-2\epsilon_2 ZJ(ab)^2]^{1/2}+ZJ(2ab)^2-\epsilon_2} \tag{28}$$

and

$$\frac{C_1^2}{C_2^2}=\frac{zJ(2ab)^2}{\epsilon_2+ZJ(2ab)^2-[\epsilon_2{}^2+2\epsilon_2 ZJ(2ab)^2]^{1/2}}\ . \tag{29}$$

The operators are properly normalized by

$$(C_1^1)^2-(C_2^1)^2=\tfrac{1}{2}\ \text{ and }\ (C_1^2)^2-(C_2^2)^2=\tfrac{1}{2}\ . \tag{30}$$

The eigenvalues are

$$\lambda_{2,1}=[\epsilon_2{}^2\pm 2\epsilon_2 zJ(2ab)^2]^{1/2}\ . \tag{31}$$

The higher-frequency mode λ_2 is easily shown to be optically active, in σ polarization only, whereas the lower-frequency mode is optically inactive.

Two parameters can be immediately extracted from a measurement of these two frequencies.

First the molecular field energy ϵ_2 is given by

$$\epsilon_2 = [\tfrac{1}{2}(\lambda_1^2 + \lambda_2^2)]^{1/2} \tag{32}$$

and the exchange parameter is determined from

$$4\epsilon_2 zJ(2ab)^2 = \lambda_2^2 - \lambda_1^2 . \tag{33}$$

We discuss this further so that we may take full advantage of these simple arguments to extract zJ. From (22) we can solve for $\alpha = zJ\langle S_z\rangle$ obtaining

$$\alpha = zJ\langle S_z\rangle = \frac{(\tfrac{1}{2}\epsilon_2)^2 - 3\gamma^2 - \delta}{\epsilon_2^2} . \tag{34}$$

We presume to know δ and γ from the diamagnetic isomorph MgF_2 and using ϵ_2 from the arithmetic mean of the squares of the Davydov states λ_1 and λ_2 [Eq. (32)] we determine α. But α taken with δ and γ determine the coefficients a, b from (21). At this point the magnetic interactions are completely specified, within the framework of this simplified model, for $\langle S_z\rangle$ is immediately determined from

$$\langle S_z\rangle = \tfrac{3}{2}a^2 - \tfrac{1}{2}b^2$$

and zJ from $\alpha/\langle S_z\rangle$. We can use the Davydov splitting in the form of (33) to immediately check on how consistent the model is, since the splitting has not been used to extract any parameters up to this point.[21]

III. EXPERIMENT

Far-infrared absorption experiments were performed on oriented single-crystal plates of CoF_2 grown by the Bridgman technique. A Michelson Fourier-transform spectrometer was used to record the spectra from 10 to 300 cm^{-1}.[22] Polarization of the radiation was achieved with grid polarizers constructed either of wires or strips of gold on Mylar. The temperature of the sample was held at 4.2 °K for most of the experiments but could be warmed and held to any desired temperature up to room temperature by means of a heater, forward biased GaAs diode thermometer, and feedback control circuit. Magnetic fields as large as 50 kG were used to measure both the linear Zeeman effect obtained with the field parallel to the c axis as well as the nonlinear splittings produced with the field perpendicular to this axis.

Essentially, all of the uniform, $k = 0$, single-particle excitations of the spin system have been observed below 300 cm^{-1}, as well as the two-particle excitations represented by the two-magnon absorption, previously reported by Richards.[23] The energies of the modes and their Zeeman effect are summarized in Fig. 4. Energies and frequencies are expressed in wave-number units. The lowest-frequency mode at 36.3 cm^{-1} is the antiferromagnetic resonance and was first reported by Richards. The data shown here are due to Richards.[2] The mode is twofold degenerate, splitting linearly in a field parallel to the c axis and nonlinearly in a field perpendicular to the c axis. As expected, polarized radiation determines that the transition is a magnetic-dipole transition polarized perpendicular to c. There are two other modes at 193 and 256 cm^{-1} that appear to have the same symmetry as the resonance at 36.3 cm^{-1}. Complete polarized radiation experiments cannot be done on the former due to the strong lattice absorption for α and σ polarization; however, its appearance in π polarization is at least consistent with a magnetic-dipole transition perpendicular to the c axis. This mode can be successfully interpreted as the transverse exciton or spin wave derived from the upper Kramers doublet of the Co^{2+} ion. It was originally observed by Barker *et al.*[1] in the infrared and by Martel *et al.*[3] with neutrons. The 256-cm^{-1} line has been discussed at length in the previous paper and is interpreted as the E_g phonon which derives its magnetic-dipole strength from the interaction with the magnetic excitations.

Neither of the Davydov split excitations is seen in zero magnetic field. On the one hand the low-frequency component at 168.5 cm^{-1} is forbidden in zero field and on the other the high-frequency mode at 210.9 cm^{-1} can be seen in σ polarization only, which is strongly absorbed by the lattice. Fortunately CoF_2 is very sensitive to magnetic fields perpendicular to the c axis, which break down the above selection rules, and enable one to see the excitations in other polarizations at least in a finite magnetic field. The frequencies quoted are those obtained by fitting the observed frequency dependence on magnetic field to a square law and extrapolating back to zero field. The zero field data are consistent with the neutron results.

For the sake of completeness, we also show the two-magnon absorption seen for $E \parallel c$ axis at 4.2 °K (Fig. 5). The shift of the relatively sharp peak away from the peak in two-magnon density of states may be accounted for by magnon-magnon interactions which lead to a resonant two-magnon bound state in the two-magnon continuum.[24]

IV. RESULTS

In this section we take the experimental results discussed briefly in Sec. III and attempt to make contact with the model and theory generated earlier. First we use the Davydov-split longitudinal excitations to determine the exchange parameter zJ. A simple test for consistency is made by determining the Davydov splitting above and below the Néel point and comparing with experiment. Second, all the magnetic excitations at $k = 0$ are calculated as a function of applied magnetic field in the three principal directions. At this point no spin-lattice

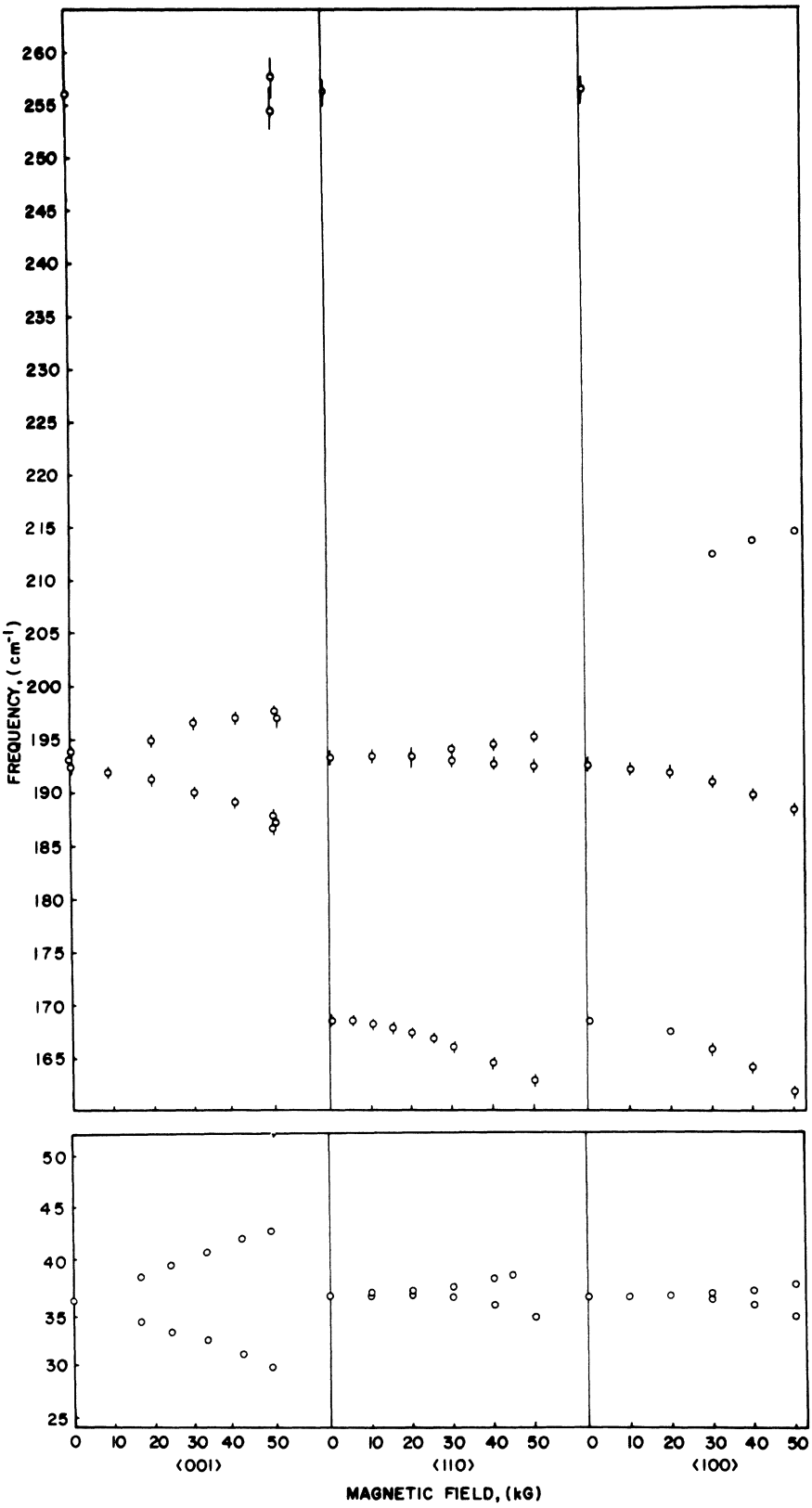

FIG. 4. Experimentally observed "single-particle" excitations at 4.2 °K and their Zeeman effect. The data for the antiferromagnetic resonance at 36.3 cm^{-1} are due to Richards (Ref. 2).

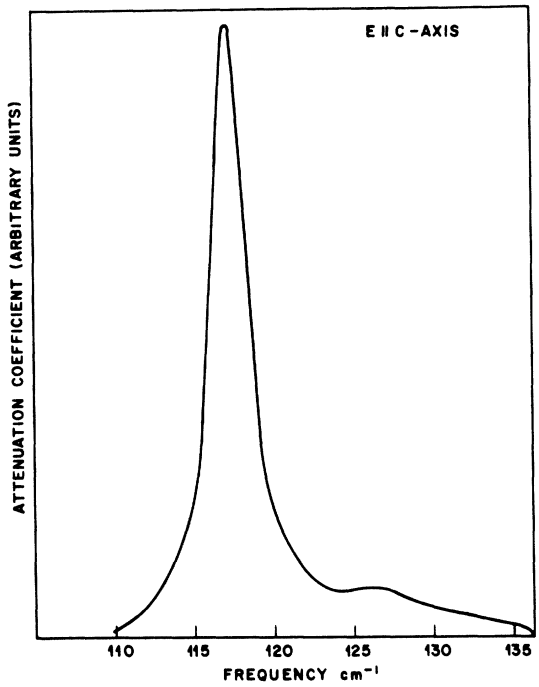

FIG. 5. Two-magnon absorption at 4.2 °K for $E \| c$ axis.

coupling is introduced and discrepancies between experiment and theory are noted for the two transverse spin-wave modes. Third, the spin-phonon coupling determined in the previous paper is included and the magnetic excitations are again calculated and compared with experiment. Fourth, the integrated intensity of the various modes is calculated and compared with experiment, and the parallel and perpendicular susceptibilities at $T = 0$ °K are obtained.

A. Longitudinal Spin-Excitations-Davydov Splitting

Using the energies of the two Davydov components $\lambda_2 = 210.9$ cm^{-1} and $\lambda = 168.5$ cm^{-1}, we can determine the molecular field splitting ϵ_2 from Eq. (32):

$$\epsilon_2 = 190.8 \text{ cm}^{-1} .$$

From Eq. (34) we solve for $\alpha = zJ\langle S_z\rangle$ by using $\delta = +24$ cm^{-1} and $\gamma = 43$ cm^{-1}, the crystal-field parameters determined from Co^{2+} in MgF_2:

$$\alpha = zJ\langle S_z\rangle = 35.6 \text{ cm}^{-1} .$$

The wave function for the molecular field ground state $|0\rangle$, $|0\rangle = a|\tfrac{3}{2}\rangle + b|-\tfrac{1}{2}\rangle$, is determined from (21)

$$a = 0.902, \quad b = 0.433 .$$

This gives

$$\langle S_z\rangle = 1.13 ,$$

which may be compared to the value of 1.25 measured by nuclear magnetic resonance (NMR).[25] We note here that no effects due to zero-point spin deviation are included in these calculations. This will have the effect of making the discrepancy between $\langle S_z\rangle$ determined from the Davydov energies and the NMR measurement slightly larger. The discrepancy although noteworthy is not unbearable. The exchange parameter is then found to be $zJ = 31.8$ cm^{-1}. This value differs by ~ 10% from the value given by Lines[7] and by 5% from the work of Belorizky *et al.*[26] on Co^{2+} pairs in MgF_2.

At this point, the magnetic interactions are completely specified and we can test to some extent the consistency of the present calculations, without proceeding much further, by asking for the Davydov splitting both above and below the Néel point. At $T = 0$ °K we use Eq. (31) and obtain

$$\lambda_2 = 209.5 \text{ cm}^{-1},$$

$$\lambda_1 = 171 \text{ cm}^{-1} ,$$

which compare satisfactorily with the experimental values

$$\lambda_2 = 210.9 \pm 1 \text{ cm}^{-1} ,$$

$$\lambda_1 = 168.5 \pm 1 \text{ cm}^{-1} .$$

Above the Néel point we must recalculate ϵ_2 and the matrix element $\langle 2|S^x|0\rangle = 2ab$. ϵ_2 is equal to 157 cm^{-1} while a and b are given by

$$a = 0.808, \quad b = 0.589 .$$

Using Eq. (31) again, we obtain, above the Néel point

$$\lambda_2 = 183 \text{ cm}^{-1} ,$$

$$\lambda_1 = 126 \text{ cm}^{-1} ,$$

as compared with the experimental values given by the neutron scattering[3]

$$\lambda_2 = 178 \pm 3 \text{ cm}^{-1} ,$$

$$\lambda_1 = 138 \pm 3 \text{ cm}^{-1} .$$

Although the agreement is not as satisfying as was obtained at $T = 4.2$ °K, the deviations are only about 5%. Although it is not clear why one has a larger discrepancy above the Néel point, we can suggest a possible source. We note that the increased Davydov splitting above the Néel point is due to the increase of the matrix element $\langle 2|S^x|0\rangle$ caused in turn by reducing the molecular field to zero. Although the average field is zero in the disordered state, at any time there will, of course, be a finite exchange field at a particular site which will both alter ϵ_2 and change the matrix element $\langle 2|S^x|0\rangle$. It is clear that this will broaden the line but it may also lead to a shift if we allow near-neighbor cor-

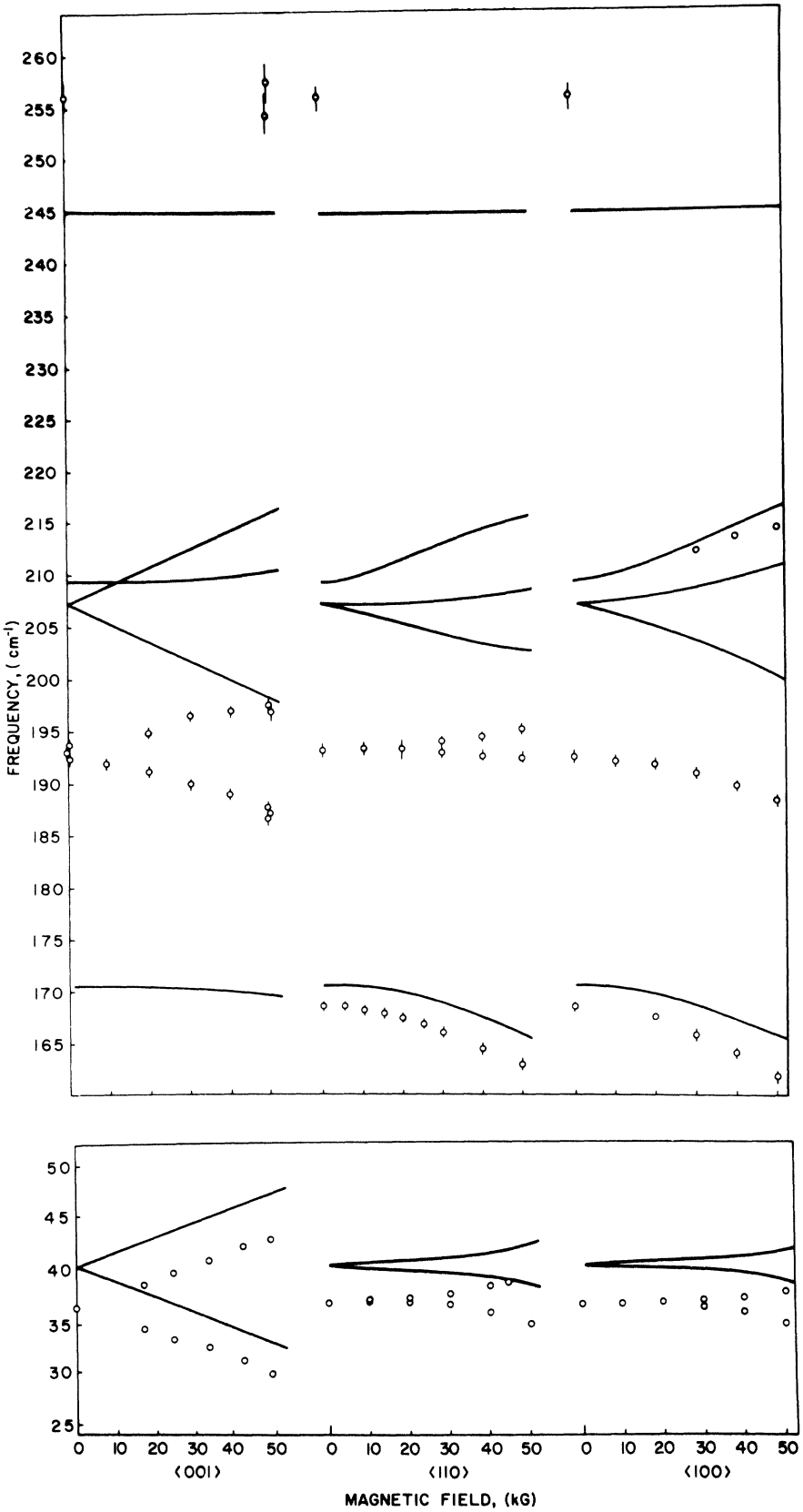

FIG. 6. Uniform magnetic excitations in the *absence* of spin-phonon coupling.

relations. We will not pursue the high-temperature results further.

The fact that the zJ extracted from the molecular field energy ϵ_2 can be used successfully to obtain the Davydov splitting implies that either the results are fortuitous or that the longitudinal excitations are relatively unencumbered by either appreciable multipole-multipole spin interactions produced by off-diagonal exchange or dynamic spin-phonon coupling. Since the discrepancy in the Davydov splitting is approximately 10%, we may infer, ignoring the possibility of a fortuitous agreement, that off-diagonal exchange and spin-phonon coupling energies for the longitudinal excitations are $\leq 10\%$ of zJ. We then proceed with only the single exchange parameter zJ ignoring off-diagonal exchange but admitting the possibility of terms $\leq 10\%$ of the simple isotropic near-neighbor exchange.

B. Spectrum of Excitations—No Spin-Phonon Coupling

Using the prescription described in Sec. IV A, we can now construct the full spectrum of uniform magnetic excitations for arbitrary magnetic field. We do so first with no spin-phonon coupling. The results along with the experimental data are shown in Fig. 6.

The most obvious discrepancy is the unperturbed E_g phonon. It is neither allowed in absorption nor does it show any magnetic field effects. It is shown at 245 cm^{-1}—the unperturbed value determined in a latter computation—and also close to the room-temperature energy determined by MacFarlane and Ushioda,[27] 246 cm^{-1}. Further we note that the high-lying transverse excitation at 207.5 cm^{-1} is approximately 15 cm^{-1} too high and the low-lying excitation of the same symmetry at 40 cm^{-1}, the antiferromagnetic resonance, is ~4 cm^{-1} too high. Further the nonlinear splitting of the high-lying mode only qualitatively agrees with the experimental result. There appears to be too much interaction with the high-frequency component of the Davydov excitations.

C. Spectrum of Excitations—Spin-Phonon Coupling

The spin-phonon coupling calculated in the first paper is introduced in a slightly underhanded way.

TABLE I. Spin-E_g phonon coupling parameters.

		Intensity E_g phonon (cm^{-1})	$k=0$, energies
I	$(\hbar/2m\omega_p)^{1/2}\eta$	17.5	19
	$(\hbar/2m\omega_p)^{1/2}\xi$	21.6	23.48
II	$(\hbar/2m\omega_p)^{1/2}\eta$	21.5	20.5
	$(\hbar/2m\omega_p)^{1/2}\xi$	−26.6	−25.35

Although the relative magnitude of the two interaction parameters η and ξ was presumed to be well determined from the shape of the intensity-versus-temperature curves, the absolute magnitude was determined by the measured integrated intensity which is known only to within 10%. The energies of the excitations are determined with considerably more precision. Consequently in fitting the energies at $k=0$, we have adjusted the magnitude of the coupling parameters while keeping the ratio constant. At the same time, the unperturbed E_g phonon frequency was adjusted simultaneously until the E_g phonon energy and the high-lying transverse spin excitation were reproduced to within 1 cm^{-1}.

To allay any suspicion at this point, we quote the spin-phonon interaction parameters obtained by such a fit and compare with those determined in the first paper. These are shown in Table I. In both cases approximately 5% discrepancies are introduced in order to fit the energies of the high-lying transverse spin wave and the E_g phonon to within 1 cm^{-1}.

The results obtained for all the $k=0$ excitations as a function of applied magnetic field are shown in Figs. 7 and 8. There is little to choose between the two sets of parameters. Parameter set I improves the agreement of the antiferromagnetic resonance by shifting it downward by ~3 cm^{-1} but does not reproduce the $\langle 100 \rangle$ magnetic field shift of the high-lying transverse excitation or the high-frequency Davydov component. Parameter set II gives good agreement for all of the Zeeman-effect data but does not perturb the antiferromagnetic resonance at 40 cm^{-1} and consequently leaves a discrepancy there of about 3.7 cm^{-1}. Both sets of parameters reproduce the splitting of the E_g phonon in an $\langle 001 \rangle$ oriented magnetic field. The experimental data also agree with an estimate of the g factor for the E_g phonon recently made by Mills and Ushioda.[28]

The zone-boundary spin-wave energy obtained in the absence of spin-phonon coupling is 56 cm^{-1}, compared with a value ~63 cm^{-1} obtained by neutron scattering.[3] No attempt has been made to obtain the zone-boundary energy with the spin-phonon coupling included but it does not appear that it could ameliorate the existing discrepancy.

D. Integrated Intensities

The matrix elements obtained by diagonalizing the Hamiltonian (15) can be used to calculate the integrated intensities of the $k=0$ modes from the following equation:

$$\int \alpha \, d\nu = \frac{2\pi^2 n \mu_0 \nu \rho}{hc} \langle M^\beta \rangle^2 \ \mathrm{cm}^{-2},$$

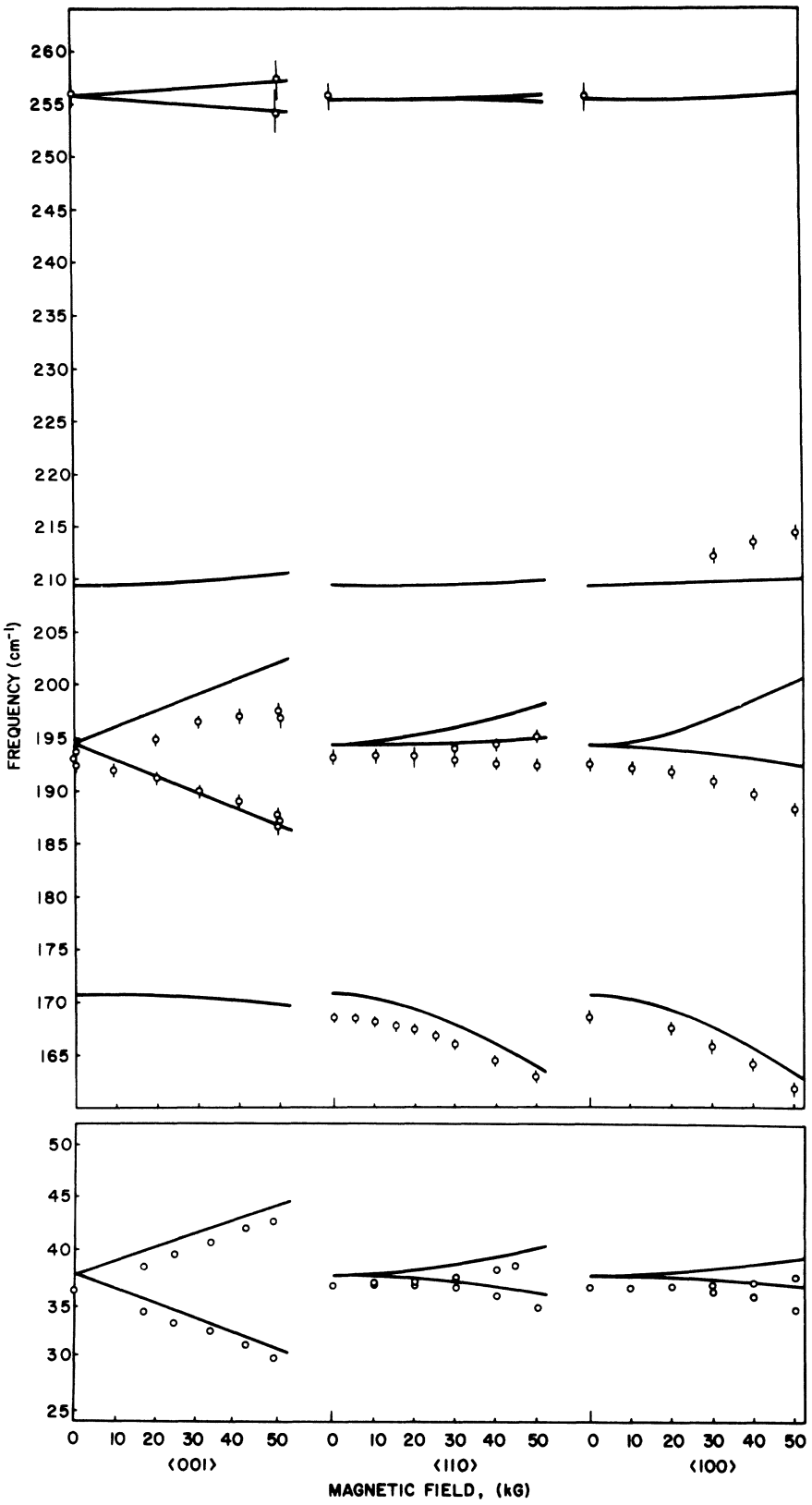

FIG. 7. Uniform magnetic excitations with the following spin-phonon coupling parameters: $(\hbar/2m\omega_p)^{1/2}\eta = 19\ \mathrm{cm}^{-1}$, $(\hbar/2m\omega_p)\xi = 23.48\ \mathrm{cm}^{-1}$.

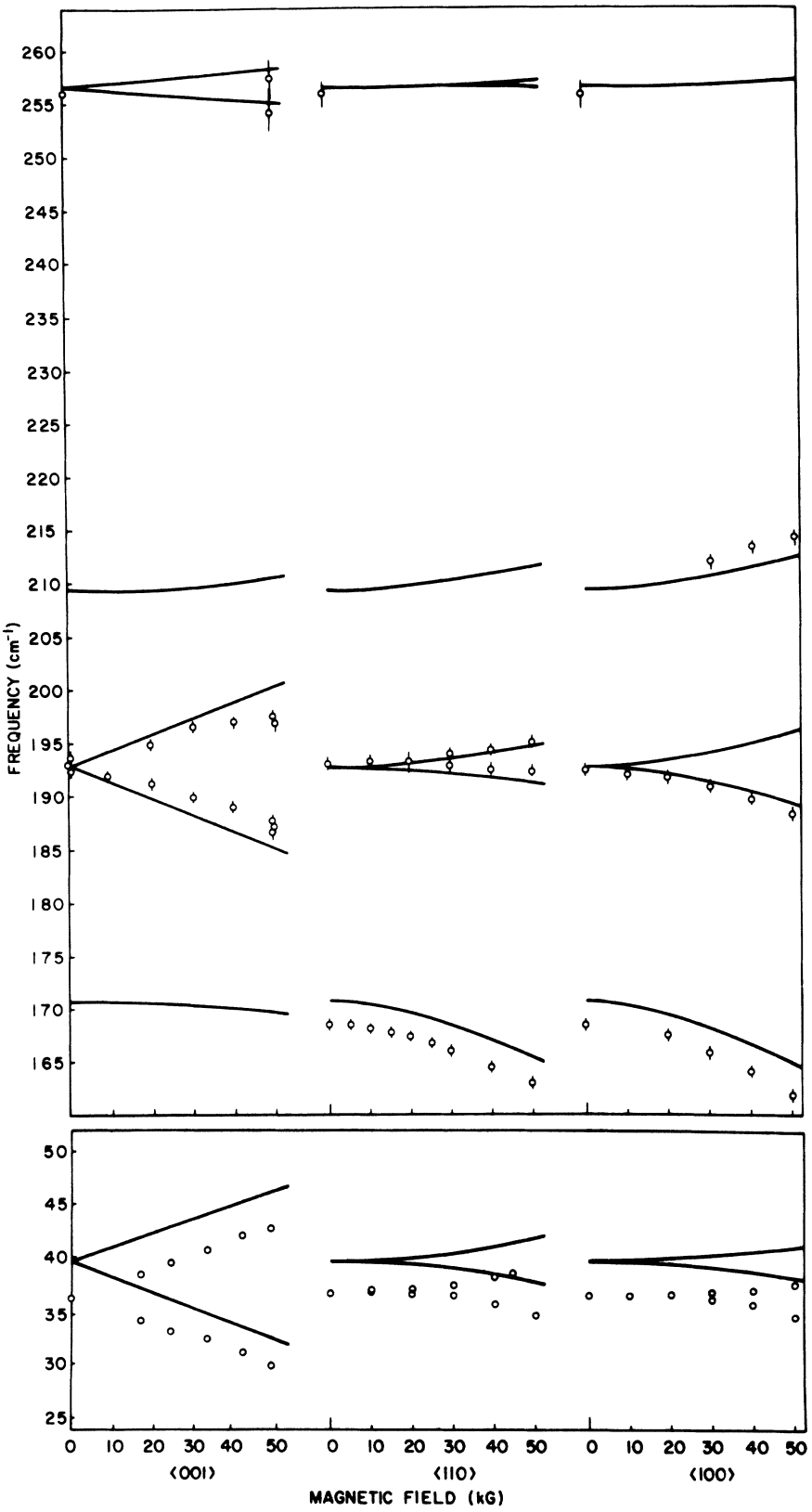

FIG. 8. Uniform magnetic excitations with the following spin-phonon coupling parameters: $(\hbar/2m\omega_p)^{1/2}\eta = 20.5\ \mathrm{cm}^{-1}$, $(\hbar/2m\omega_p)^{1/2}\xi = -25.35\ \mathrm{cm}^{-1}$.

TABLE II. Integrated intensity. $zJ=31.8$; $\delta=-24$; $\gamma=43$; $g_z=2.6$; $g_y=2.6$; $g_x=1.8$; $\hbar\omega_p=245$; $\eta=19$; $\xi=23.48$.

Frequency cm^{-1}		Axial		π	Intensity $\int\alpha\,d\nu$ cm^{-2}	σ	
Expt	Theor	Expt	Theor	Expt	Theor	Expt	Theor
36.3	37.6	900±90	1100		1000	0	0
168.5	170.6	0	0	0	0	0	0
193	194.4	···	···	660±45	860	···	···
210.9	209.5	···	···	0	0	···	···
256	255.7	440±40	285		500	0	0

where n is the index of refraction taken from Barker and Ditzenburger[1]; μ_0 is the mks permeability of free space, $4\pi\times10^{-7}$; ρ is the reciprocal of unit-cell volume, mks units; ν is the resonant frequency in cm^{-1}; h is Planck's constant, mks units; c is the speed of light in cm/sec; $\langle M^\beta\rangle^2$ is the square magnitude per unit cell of the total magnetic moment operator in the β direction; β specifies the direction of the infrared magnetic field.

The results for zero applied magnetic field are collected in Tables II and III. The entries marked with an asterisk are inaccessible since they lie in the reststrahl band for E perpendicular to the c axis. Although the intensity of the antiferromagnetic resonance agrees reasonably well with the theory for both sets of parameters, the intensity of the high-lying spin-wave mode at 193 cm^{-1} and the E_g phonon is less encouraging. There are approximately 50% discrepancies in both values and the sign of the discrepancy indicates that not enough intensity has been transferred from the spin-wave mode to the E_g phonon. It is noted rather strongly at this point, that for a given energy perturbation of the two modes in question, different transferred intensity may be obtained by altering the relative size of η and ξ. For instance, in data shown in Table II decreasing η by 25% and increasing ξ by the same does not impair the agreement with the energies but does increase the E_g intensity to 380 cm^{-2} and decrease the high-lying spin-wave intensity to 750 cm^{-1}. This indicates that the spin-phonon coupling parameters extracted from the analysis in the preceding paper may be in error by as much as 30%.

With a magnetic field applied to the sample in a $\langle110\rangle$ direction or a $\langle100\rangle$ direction the lower component of the longitudinal spin excitations becomes allowed with an integrated intensity that increases quadratically with magnetic field. The experimental data as well as the theoretical dependence for a $\langle110\rangle$-directed field are shown in Fig. 9. The agreement is satisfactory for either parameter set.

We may also note some qualitative features of the absorption intensity versus magnetic field perpendicular to the spin axis, which hold for either set of parameters. For a $\langle100\rangle$-directed field and radiation propagating in the $\langle100\rangle$ direction, the calculation indicates that only the high-lying mode of the antiferromagnetic resonance at 36.3 cm^{-1} should be seen. Richards[2] indicates that the intensity of the high-frequency component to low-frequency component is ~ 10/1. For the high-lying transverse excitation at 193 cm^{-1}, the reverse is expected—only the low-frequency component should be seen. This is verified experimentally.

For a $\langle110\rangle$-directed magnetic field and propagation vector, the calculation indicates that the low-frequency component of the 36.3-cm^{-1} mode is three orders of magnitude stronger than the high-frequency component. Richards[2] observes a ratio of ~ 10/1. For the 193-cm^{-1} modes the calculation shows that low-frequency component should be stronger by two orders of magnitude whereas the reverse is obtained experimentally with a ratio of ~ 5/1. With the exception of the latter, the results of the calculation agree at least qualitatively with experiment. Quantitative agreement, at least for the high-intensity ratios, could only be tested with well-collimated radiation. Precautions of this

TABLE III. Integrated intensity. $zJ=31.8$; $\delta=-24$; $\gamma=43$; $g_z=2.6$; $g_y=2.6$; $g_x=1.8$; $\hbar\omega_p=245$; $\eta=20.5$; $\xi=-25.35$.

Frequency cm^{-1}		Axial		Intensity cm^{-2} π		σ	
Expt	Theor	Expt	Theor	Expt	Theor	Expt	Theor
36.3	39.7	900±90	1070		980	0	0
168.5	170.6	0	0	0	0	0	0
193	192.8	···	···	660±45	860	···	···
210.9	209.5	···	···	0	0	···	···
256	256.6	440±40	285		500	0	0

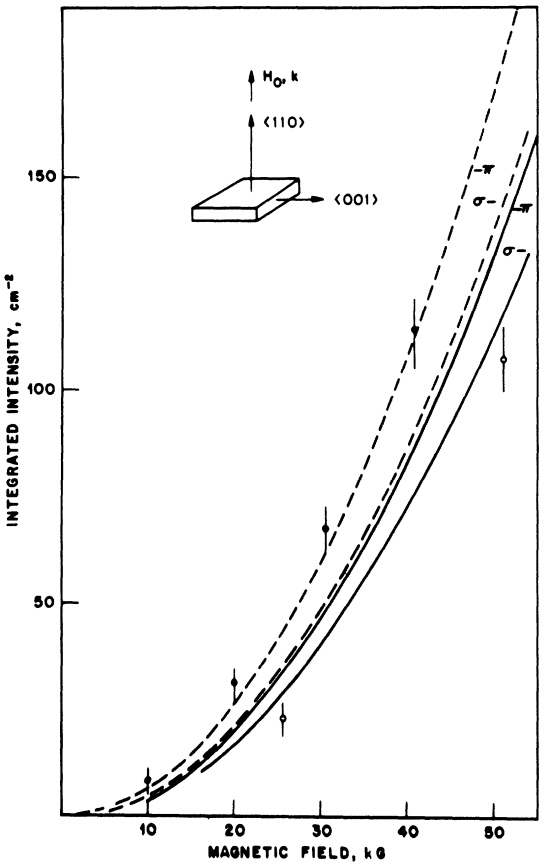

FIG. 9. Intensity of optically inactive Davydov component as a function of magnetic field in (110) directions. ●—π polarization; ○—σ polarization.

Solid line:	Dashed line:
$(\hbar/2m\omega_p)^{1/2}\eta = 19\ \mathrm{cm}^{-1}$,	$(\hbar/2m\omega_p)^{1/2}\eta = 20.5\ \mathrm{cm}^{-1}$,
$(\hbar/2m\omega_p)^{1/2}\xi = 23.48\ \mathrm{cm}^{-1}$.	$(\hbar/2m\omega_p)^{1/2}\xi = -25.35\ \mathrm{cm}^{-1}$.

sort were not taken in any of the above experiments.

E. Parallel and Perpendicular Susceptibility

The self-consistent ground state for applied magnetic fields parallel and perpendicular to the spin direction immediately determine the $T = 0\,^\circ\mathrm{K}$ susceptibility. We obtain

$$\chi_\perp(\mathrm{calc}) = 615\times 10^{-6}\ \mathrm{emu/g}\ ,$$

$$\chi_\parallel(\mathrm{calc}) = 105\times 10^{-6}\ \mathrm{emu/g}\ ,$$

whereas Foner[29] has observed

$$\chi_\perp(\mathrm{expt}) = 600\times 10^{-6}\ \mathrm{emu/g}\ ,$$

$$\chi_\parallel(\mathrm{expt}) = 100\times 10^{-6}\ \mathrm{emu/g}\ .$$

The agreement is satisfactory.

V. DISCUSSION

A quantitative description of the uniform magnetic excitations in CoF_2, at low temperatures, below 300 cm^{-1}, can be obtained by including the spin-E_g optical-phonon coupling in an otherwise simple model for the magnetic interactions. It should be noted that in this fit we have had only one parameter at our disposal, the isotropic exchange between effective $S = \frac{3}{2}$ spins. The energies have been reproduced at $k = 0$ to within ~ 3% and the linear and nonlinear Zeeman effects are satisfactorily reproduced by the model. It would appear that off-diagonal exchange and the concomitant multipolar spin interactions are not important in the excitations we have considered. Off-diagonal exchange would manifest itself in the nonlinear Zeeman effect or by preventing a single-exchange parameter fit to the excitation energies. Agreement between the model and experiment is not perfect but the existing discrepancies are probably not inconsistent with our estimates of the strength of the multipolar terms, $\sim 0.03zJ$.

The integrated absorption intensities are the least satisfactory. Most noteworthy is the discrepancy between the measured and calculated intensities of the E_g phonon and the high-lying transverse excitation. This indicates that although the total interaction between the E_g phonon and the spin system is correct, the relative contributions of the two possible local lattice distortions may be in error by as much as 30%.

ACKNOWLEDGMENTS

The authors would like to acknowledge useful discussions with R. E. Dietz, G. Parisot, P. Martel, R. A. Cowley, R. M. MacFarlane, T. Moriya, and R. Loudon. L. R. Walker was particularly helpful in suggesting the method of diagonalizing the Hamiltonian. They would like to thank P. L. Richards for the use of his unpublished data on the antiferromagnetic resonance. F. DeRosa is gratefully acknowledged for his technical assistance. The computer program for diagonalizing non-Hermitian matrices was provided by P. Businger.

APPENDIX A: OFF-DIAGONAL EXCHANGE

We consider the exchange interaction between two Co^{2+} ions shown in Fig. 10. The symmetry of the pair, determined by the intervening fluorine ligand, contains a single reflection in the plane of the bond, i.e., the zy plane in Fig. 10. The three relevant orbital states on each site are also shown in Fig. 11. Translating from the A site to the B site necessitates a rotation of 90° about the z axis. This is reflected in the interchange of the $|y\rangle$ and $|x\rangle$ states on the two different sites.

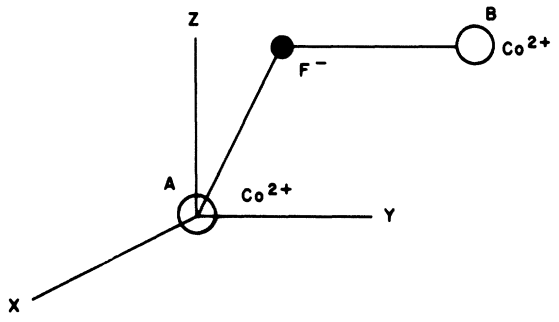

FIG. 10. Symmetry of a pair of interacting Co^{2+} ions.

Associated with each of these levels is a fourfold spin degeneracy which we represent by an effective $S=\frac{3}{2}$ spin on each of the sites, $\vec{S}^A$ and $\vec{S}^B$.

We now treat the perturbation of the ground state by the spin-orbit interaction and off-diagonal exchange. The perturbing Hamiltonian is the following:

$$H' = \lambda\vec{L}^A\cdot\vec{S}^A + \lambda\vec{L}^B\cdot\vec{S}^B + \sum_{\alpha,\beta;\gamma,\delta} J\begin{pmatrix}\alpha & \gamma\\ \beta & \delta\end{pmatrix}\vec{S}^A\cdot\vec{S}^B + K\begin{pmatrix}\alpha & \gamma\\ \beta & \delta\end{pmatrix}, \quad \text{(A1)}$$

where λ is the spin-orbit coupling and $\vec{L}$ is an effective $l=1$ operator in the Γ_4 manifold. λ is in fact an effective spin-orbit coupling parameter for the $L=1$ operator in the Γ_4 manifold. If it were not for the weak mixing of the ^4F state with the ^4P state by the cubic field $\lambda=-\frac{3}{2}\Lambda$, where Λ is the appropriate spin-orbit parameter for the ^4F manifold of Co^{2+} in MgF_2. Λ should be close to but different from the free-ion value for the ^4F state. According to Gladney[11] $\lambda\sim-1.43\Lambda$ and $\Lambda\sim-157$ cm^{-1} about 10% reduced from the free-ion value for the ^4F state of 178 cm^{-1}.

The exchange parameter $J(^{\alpha\ \gamma}_{\beta\ \delta})$ describes off-diagonal exchange between the A and B sites. We change the orbital state on site A from $|\alpha\rangle$ to $|\beta\rangle$ and the orbital state on B from $|\gamma\rangle$ to $|\delta\rangle$.[30] $K(^{\alpha\ \gamma}_{\beta\ \delta})$ describes a similar simultaneous change in orbital states but is spin independent. If we may describe the exchange as being either pure kinetic or potential exchange, then $K(^{\alpha\ \gamma}_{\beta\ \delta})$ reduces to either $\frac{1}{4}n^2J(^{\alpha\ \gamma}_{\beta\ \delta})$ or $-\frac{1}{4}n^2J(^{\alpha\ \gamma}_{\beta\ \delta})$, respectively, where n is the number of electrons or holes on the magnetic ion being exchanged.[30,31] In this case $n=3$. For an unknown mixture of kinetic and potential exchange, the relationship between K and J is unspecified. In the following we ignore K since we are interested only in the spin-dependent part of the perturbation.

In the absence of any symmetry at the pair, there are 45 different exchange parameters.[32] Since the plane containing the fluorine bond is a reflection plane, 20 of these parameters must be zero. The remaining 25 may participate in the perturbation calculation.

We now proceed via perturbation theory to find the ground orbital state of the pair as a function of $\vec{S}^A$ and $\vec{S}^B$ with λ and J as expansion parameters. There is only one diagonal matrix element of H' in the ground orbital state for the representation shown in Fig. 11. It is the simple isotropic diagonal exchange used in the paper:

$$J\begin{pmatrix}x & y\\ x & y\end{pmatrix}\vec{S}^A\cdot\vec{S}^B. \quad \text{(A2)}$$

The largest second-order terms are those in λ^2 and generate the orthorhombic crystal field for the effective $S=\frac{3}{2}$ states:

$$-\left(\frac{\lambda^2}{E_2}-\frac{1}{2}\frac{\lambda^2}{E_1}\right)[(S_z^A)^2+(S_z^B)^2]-\frac{\lambda^2}{E_1}[S(S+1)] + \frac{\lambda^2}{2E_1}[(S_x^A)^2-(S_x^A)^2]-\frac{\lambda^2}{2E_1}[(S_x^B)^2-(S_y^B)^2]. \quad \text{(A3)}$$

[It should be noted here that there are single-ion terms of the order of $zJ\lambda^2/E^2$ which effectively change the magnitude of the anisotropy field in (A3). Since they are zJ/E times the terms in (A3), they are probably only ~ 5% corrections and indistinguishable from real changes in the crystal-field terms produced by changing the host from MgF_2 to pure CoF_2. These exchange-induced corrections in crystal field may be viewed as a change in effective spin-orbit parameter, on a given site, when it is interacting via off-diagonal exchange, with neighboring orbitally degenerate ions.[33,34]] Also of second order but less important is a single term in λJ—the Moriya-Dzialoshinski antisymmetric exchange[13]:

$$\frac{\lambda}{E_1}J\begin{pmatrix}x & y\\ x & z\end{pmatrix}\hat{i}_x\cdot(\vec{S}^A\times\vec{S}^B). \quad \text{(A4)}$$

The total symmetry of CoF_2 prevents this term from contributing anything to the uniform excitations of the system. Terms second order in J are

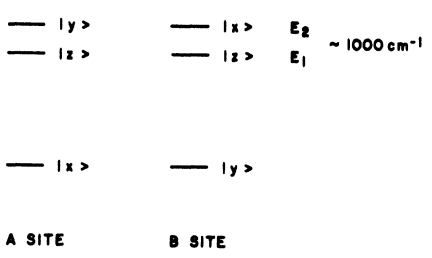

FIG. 11. Splitting of the Γ^4 orbital ground state of Co^{2+} by the orthorhombic crystal field.

of no consequence—for that matter any term involving J/E rather than λ/E may be safely neglected.

The first interesting multipolar spin interaction terms appear in third order, second order in λ, first order in J. The terms that arise are many and we write only a typical one here:

$$-\frac{\lambda^2}{E_2^2}\left\{\left[J\begin{pmatrix}x & y\\ x & y\end{pmatrix}-J\begin{pmatrix}x & x\\ x & x\end{pmatrix}\right]\vec{S}^A\cdot S_z^B\vec{S}^B S_z^B + \left[J\begin{pmatrix}x & y\\ x & y\end{pmatrix}-J\begin{pmatrix}y & y\\ y & y\end{pmatrix}\right]\vec{S}^B S_z^A\vec{S}^A S_z^A\right\}. \quad \text{(A5)}$$

If we restrict our discussion to the uniform response of the system, we simply sum interactions of the form (A5) over all the neighbors at the corners of the unit cell to find the total interaction between the two sublattices that has the same form as (A5). We obtain

$$-\frac{\lambda^2}{E_2^2}\left\{zJ\begin{pmatrix}x & y\\ x & y\end{pmatrix}-\frac{1}{2}\left[zJ\begin{pmatrix}x & x\\ x & x\end{pmatrix}+zJ\begin{pmatrix}y & y\\ y & y\end{pmatrix}\right]\right\} \times(\vec{S}^A\cdot S_z^B\cdot\vec{S}^B S_z^B+\vec{S}^B\cdot\vec{S}_z^A\vec{S}^A S_z^A). \quad \text{(A6)}$$

For the sake of completeness we write all the spin interactions up to second order in λ^2 and first order in J which contribute to the uniform excitations:

Single-ion anisotropy

$$-\frac{\lambda^2}{E_2}(S_z^A)^2-\frac{\lambda^2}{E_2}(S_z^B)^2-\frac{\lambda^2}{E_1}(S_y^A)^2-\frac{\lambda^2}{E_1}(S_x^B)^2. \quad \text{(A7)}$$

Bilinear exchange

$$zJ\begin{pmatrix}x & y\\ x & y\end{pmatrix}\vec{S}^A\cdot\vec{S}^B-zJ\begin{pmatrix}x & y\\ x & y\end{pmatrix}\frac{\lambda^2}{E_1^2}S_z^A S_z^B -\left\{zJ\begin{pmatrix}x & y\\ x & y\end{pmatrix}\left(\frac{\lambda^2}{2E_1^2}+\frac{\lambda^2}{E_2^2}\right) +\frac{1}{2}\frac{\lambda^2}{E_2^2}\left[zJ\begin{pmatrix}x & y\\ y & x\end{pmatrix}+zJ\begin{pmatrix}x & x\\ y & y\end{pmatrix}\right]\right\}(S_x^A S_x^B+S_y^A S_y^B). \quad \text{(A8)}$$

Quadrupole-quadrupole

$$\frac{\lambda^2}{E_2^2}\left[zJ\begin{pmatrix}x & y\\ y & x\end{pmatrix}-zJ\begin{pmatrix}x & x\\ y & y\end{pmatrix}\right] \times[2Q_{zz}^A Q_{zz}^B+\tfrac{1}{2}(Q_{zx}^A Q_{zx}^B+Q_{zy}^A Q_{zy}^B)]. \quad \text{(A9)}$$

Dipole-octupole

$$+\frac{\lambda^2}{E_2^2}\left\{\frac{1}{2}\left[zJ\begin{pmatrix}x & x\\ x & x\end{pmatrix}+zJ\begin{pmatrix}y & y\\ y & y\end{pmatrix}\right]-J\begin{pmatrix}x & y\\ x & y\end{pmatrix}\right\} \times(\vec{S}^A S_z^B\vec{S}^B S_z^B+\vec{S}^B S_z^A\vec{S}^A S_z^A)$$

$$+\frac{\lambda^2}{E_1^2}\left\{\frac{1}{2}\left[zJ\begin{pmatrix}x & z\\ x & z\end{pmatrix}+zJ\begin{pmatrix}z & y\\ z & y\end{pmatrix}\right]-J\begin{pmatrix}x & y\\ x & y\end{pmatrix}\right\} \times(\vec{S}^A S_y^B\vec{S}^B S_y^B+\vec{S}^B S_y^A\vec{S}^A S_y^A$$

$$+\vec{S}^A S_x^B\vec{S}^B S_x^B+\vec{S}^B S_x^A\vec{S}^A S_x^A). \quad \text{(A10)}$$

In the limit where all the J's are equal, all of the multipolar terms vanish and the remaining anisotropy in the bilinear term proves to be small, $\sim 0.06zJ$ when the appropriate parameters are introduced.

APPENDIX B: MAGNETOELASTIC CONTRIBUTION TO NONLINEAR ZEEMAN EFFECT

We make a crude estimate in this section of the contribution of the magnetoelastic coupling to the nonlinear Zeeman effect by calculating the magnetoelastic free energy for an applied magnetic field perpendicular to the spin direction. We assume a classical model of the spin and lattice and write the following expression for the energy:

$$E=\tfrac{1}{2}cu^2+ku(Q_{zx}^A+Q_{zx}^B)+zJ\vec{S}^A\cdot\vec{S}^B -g\mu_B(S_x^A+S_x^B)H_0, \quad \text{(B1)}$$

where u is the lattice strain, c the elastic constant, k the quadrupole-lattice coupling constant, zJ the exchange energy, and H_0 the applied magnetic field. The field H_0 will deviate the spins by a small angle θ from the preferred axis (z axis). Then we have for small θ

$$Q_{zx}^A=Q_{zx}^B\sim S^2\theta, \qquad S_x^A=S_x^B\sim S\theta, \qquad \vec{S}^A\cdot\vec{S}^B\sim-(1-2\theta^2)S^2, \quad \text{(B2)}$$

and

$$E(u,\theta)=\tfrac{1}{2}cu^2+ku\theta S^2+zJS^2(-1+2\theta^2)-2g\mu_B H_0\theta S. \quad \text{(B3)}$$

The equilibrium lattice distortion is given simply by

$$\frac{\partial E}{\partial u}=0, \qquad u=-\frac{kS^2\theta}{c}. \quad \text{(B4)}$$

Then the energy as a function of θ is

$$E=-zJS^2+2zJS^2\theta^2-\frac{1}{2}\frac{k^2S^4}{c}\theta^2-2g\mu_B SH_0\theta. \quad \text{(B5)}$$

It is clear then that the magnetoelastic coupling reduces the exchange energy by the following factor:

$$1-\frac{1}{4}\frac{k^2S^2}{c}\frac{1}{zJ}. \quad \text{(B6)}$$

The energy k^2/c can be easily shown to be of the order $2\eta^2(\hbar/2m\omega_p)/\hbar\omega_p$ where η and $\hbar\omega_p$ are the parameters used in Eq. (2). This gives

$$\frac{1}{4}\frac{k^2S^2}{c^2} \sim \frac{1}{2}\frac{\eta^2\hbar/2m\omega_p}{\hbar\omega_p} \sim 2\ \text{cm}^{-1}\ . \tag{B7}$$

But zJ is of the order of 60 cm^{-1}; hence, the magnetoelastic coupling alters the effective exchange parameter that one might use to calculate the spin configuration in a perpendicular magnetic field by approximately 3% in CoF_2. These corrections are neglected in the calculations performed in the main body of the paper.

[1]A. S. Barker and J. A. Ditzenberger, Solid State Commun. 3, 131 (1965).

[2]P. L. Richards, J. Appl. Phys. 35, 850 (1964); and unpublished.

[3]R. A. Cowley, P. Martel, and R. W. H. Stevenson, Phys. Rev. Letters 18, 162 (1967); P. Martel, R. A. Cowley, and R. W. H. Stevenson, Can. J. Phys. 46, 1355 (1968).

[4]R. W. MacFarlane, Phys. Rev. Letters 25, 1454 (1970).

[5]R. Silberglitt and J. B. Torrance, Jr., Phys. Rev. B 2, 772 (1970).

[6]H. Kamimura, J. Appl. Phys. 35, 844 (1964).

[7]M. E. Lines, Phys. Rev. 137, A982 (1965).

[8]A. Ishikawa and T. Moriya, J. Phys. Soc. Japan (to be published).

[8]S. J. Allen, Jr. and H. J. Guggenheim, Phys. Rev. Letters 21, 1807 (1968).

[10]R. A. Erickson, Phys. Rev. 90, 779 (1953).

[11]H. M. Gladney, Phys. Rev. 146, 253 (1966).

[12]L. F. Johnson, R. E. Dietz, and H. J. Guggenheim, Appl. Phys. Letters 5, 21 (1964).

[13]J. H. Van Vleck, J. Phys. Radium 12, 262 (1951); K. W. H. Stevens, Rev. Mod. Phys. 25, 166 (1953); T. Moriya and K. Yosida, Progr. Theoret. Phys. (Kyoto) 9, 663 (1953); P. M. Levy, Phys. Rev. Letters 20, 1366 (1968); Phys. Rev. 147, 311 (1966); 135, A155 (1964); R. J. Elliot and M. F. Thorpe, J. Appl. Phys 39, 802 (1968); R. J. Birgeneau, M. T. Hutchings, J. M. Baker, and J. D. Riley, J. Appl. Phys. 40, 1070 (1969), and references contained therein.

[14]T. Moriya, Phys. Rev. 120, 91 (1960); I. Dzialoshinski, J. Phys. Chem. Solids 4, 241 (1958).

[15]M. Born and K. Huang, *Dynamical Theory of Crystal Lattices* (Oxford U. P., London, 1954), p. 129 ff.

[16]We could in principle calculate the static magnetoelastic coupling constants if we had a complete and accurate description of the lattice dynamics for CoF_2 and assumed that the spin interacted solely with the internal distortions, i.e., the near-neighbor fluorine displacements.

[17]B. Grover, Phys. Rev. 137, A982 (1965).

[18]S. V. Tyablikov, *Methods in Quantum Theory of Magnetism* (Plenum, New York, 1967), p. 97 ff.

[19]P. Businger, Numerical Mathematics Program Library Project, Vol. 1, 1968 (unpublished).

[20]J. W. Allen, R. M. MacFarlane, and R. L. White, Phys. Rev. 179, 523 (1969); J. P. van der Ziel, Phys. Rev. Letters 18, 237 (1967).

[21]The model can be put to a further test at this point by asking for the Davydov splitting in the paramagnetic state. In this case $\alpha = 0$; ϵ_2, a, and b are immediately given by δ and γ, parameters taken from MgF_2, and the modes given by Eq. (31). The exchange parameter zJ should be the same in the paramagnetic state as the ordered state.

[22]P. L. Richards, J. Opt. Soc. Am. 54, 1474 (1964).

[23]P. L. Richards, J. Appl. Phys. 38, 1500 (1967); Bull. Am. Phys. Soc. 10, 33 (1965).

[24]M. F. Thorpe, J. Appl. Phys. 41, 892 (1970); R. J. Elliot and M. F. Thorpe, J. Phys. C 2, 1630 (1969).

[25]V. Jaccarino, Phys. Rev. Letters 2, 163 (1959).

[26]E. Belorizky, S. C. Ng, and T. G. Phillips, Phys. Rev. 181, 4676 (1969).

[27]R. M. MacFarlane and S. Ushioda, Solid State Commun. 8, 1081 (1970).

[28]D. L. Mills and S. Ushioda, Phys. Rev. B 2, 3815 (1970).

[29]S. Foner, quoted by M. E. Lines (Ref. 7).

[30]R. J. Elliot and M. F. Thorpe, J. Appl. Phys. 39, 802 (1968).

[31]P. W. Anderson, in *Magnetism*, edited by G. T. Rado and H. Suhl (Academic, New York, 1963), Vol. 1, p. 25.

[32]P. M. Levy, Phys. Rev. 177, 509 (1969). Equation (51) with $l_> = l_< = 1$; $[l] = 2l + 1$.

[33]P. M. Levy and G. M. Copland, Phys. Rev. 180, 439 (1969).

[34]G. M. Copland and P. M. Levy, Phys. Rev. B 1, 3043 (1970).